

# On the power law and quadratic forms for representing the leakage-pressure relationship- Case studies of sheltered chambers

Xiaofeng Zheng\*<sup>1</sup>, Christopher J Wood<sup>1</sup>

<sup>1</sup> Buildings, Energy and Environment Research Group, Faculty of Engineering, University of Nottingham, University Park, Nottingham NG7 2RD, UK

\*Corresponding author: [xiaofeng.zheng@nottingham.ac.uk](mailto:xiaofeng.zheng@nottingham.ac.uk)

## Abstract

The leakage characteristics of a building can be described by a leakage-pressure relationship, which sometimes is referred to as flow-pressure relationship. This relationship provides the leakage rate through the building envelope when it is subject to a certain pressure difference across it and this can be represented by a mathematical equation. The most widely used form is a power law equation, which gives a good empirical description of this relationship. However, an alternative in the form of a quadratic equation is preferred by some researchers for various reasons. The pros and cons of both equations have been compared and discussed for a number of years. The argument usually lies in the accuracy of the equations in representing the flow at low pressures. This paper aims to interpret the theoretical understanding of the envelope flow from the fluid mechanics' perspective and provide some insight as to how both equations perform when predicting the leakage flow at low pressures using test data obtained in sheltered environments. The accuracy of the predicted leakages at low pressures is then assessed by comparing them with directly measured values. It was found that both equations provide good curve fitting to the measurements. However, the power law equation gave slightly more accurate predictions (by up to 6%) on the leakage at low pressures than the quadratic equation in most scenarios in this study.

## Keywords

Building airtightness; Power law; Quadratic; Mathematical representation; Leakage-pressure relationship

## NOMENCLATURE

Symbol

$a, b$	Coefficients of quadratic equation
$C$	Flow coefficient ( $\text{m}^3 \cdot \text{s}^{-1} \cdot \text{Pa}^{-n}$ )
$d$	Diameter of opening (m)
$D_h$	hydraulic diameter (m)
$l$	Depth of opening (m)
$m$	A factor in acceleration term in eq.(1)
$n$	Pressure exponent in eq.(5)
$\Delta P$	Building pressure (Pa)
$Q$	Air leakage rate ( $\text{m}^3/\text{s}$ )
$Q_m$	Measured air leakage rate ( $\text{m}^3/\text{s}$ )
$Q_p$	Predicted air leakage rate ( $\text{m}^3/\text{s}$ )
$\hat{P}$	Dimensionless pressure
$S$	Resistance coefficient

$S_i$	Resistance coefficient in the $i^{\text{th}}$ leakage pathway
$u$	Flow velocity (m/s)

*Greek letter*

$\mu$	Viscosity (Pa·s)
$\rho$	Liquid density, (kg/m <sup>3</sup> )
$\gamma$	Specific heat ratio of air, 1.4
$\zeta$	Flow resistance coefficient of components such as bend, constriction and expansion, etc.
$\lambda$	Darcy friction factor
$\nu$	Kinematic viscosity, (m <sup>2</sup> /s)
$\delta E$	Measurement error of leakage rate, (%)
$\delta F$	Measurement error of fan flow rate, (%)
$\delta G$	Combined error of model and building pressure measurement, (%)
$\delta M$	Error due to modelling specification, (%)
$\delta p$	Accuracy of building pressure sensor, (%)
$\delta q$	overall error in obtaining the leakage rate, (%)

## 1. INTRODUCTION

As an important indicator of build quality and building energy performance, the building airtightness, which fundamentally determines the infiltration-caused building energy losses, has been one of the focuses in the fields of building performance research since 1970s [1]. The term ‘air leakage’, another way of quantifying airtightness, has often been used to describe the integrity of the building envelope. It fundamentally determines the building infiltration rate, which is responsible for a significant amount of energy losses during heating or cooling the building [2, 3, 4, 5, 6, 7, 8, 9, 10, 11, 12]. In the long term, it also affects the indoor air quality and building durability [13, 14]. Therefore, the measurement of building air leakage is an important procedure that allows us to understand this building property and its impact on the building operation, which informs us to take necessary measures to achieve the desired fabric airtightness and determine the right ventilation strategy for a healthy and comfortable indoor environment in an energy saving way. The building leakage characteristic is usually described by a leakage-pressure relationship that enables us to quantify the amount of air flowing through the building envelope at the pressure of interest. This relationship comes in a mathematical form that provides the context for us to gain analytical understanding of practical measurements.

The power law equation is the most widely adopted mathematical form for representing the relationship of the flow through building leaks and the corresponding pressure difference that the building envelope is subject to. It is able to provide a reasonably good empirical description of this relationship, but some researchers [1, 20] think it does not correspond to any physical paradigm. Due to the nature of leakage pathways present in the envelope of typical buildings, it is reasonable to think that the flow through the building envelope is not purely a single type of flow, but rather a mixture of multiple types of flows, for which developing laminar flow in short pipes was a preferred equivalence [15]. Standard techniques were utilised by Sherman [1, 15] to characterise this problem and come up with the same form of equation with other authors [16, 17, 18] by linearizing the Navier-Stokes equation. The pressure difference ( $\Delta P$ ) through the pipe where the flow occurs consists of the pressure drop associated with friction losses and acceleration of the fluid, which is mathematically represented by eq.(1):

$$\Delta P = \frac{128\mu l}{\pi d^4} Q + \frac{8\rho m}{\pi^2 d^4} Q^2 \quad [15] \quad (1)$$

Where,  $Q$  is the corresponding flow driven by established  $\Delta P$ ,  $m^3/s$ ;  $l$  and  $d$  are the pipe length and diameter,  $m$ ;  $\rho$ ,  $\mu$  and  $m$  are the air density ( $kg/m^3$ ), viscosity ( $Pa \cdot s$ ) and acceleration factor, respectively.

Hence, the flow through the pipe and the corresponding pressure drop has a quadratic relationship. However, a power law relationship can also be obtained as described by eq.(2) when the pressure becomes a dimensionless form as given by eq.(3):

$$Q = \hat{P}^n \quad [15] \quad (2)$$

Where,  $\hat{P}$  is a dimensionless pressure,  $n$  is the pressure exponent;

$$\hat{P} = \frac{m\rho d^4}{4096\mu^2 l^2} \Delta P \quad [15] \quad (3)$$

Where,  $n$  is also determined by the dimensionless pressure as described by eq.(4);

$$n = \frac{1}{2} (1 + (1 + 8\hat{P})^{-\frac{1}{2}}) \quad [15] \quad (4)$$

Therefore, the flow through short pipes can be described by both power law and quadratic equations and the flow regime is respectively indicated by the weight of friction term and acceleration term in eq.(1) and the  $n$  value in eq.(2).

There have been debates on the suitability of the equations on representing the leakage-pressure relationship for a number of years [19, 20, 21, 22, 23, 24, 25]. Etheridge [20] believed the quadratic equation is more accurate and easier to use than the power law and it also gives an accurate representation of the envelope flow over a wide range of pressures. Etheridge [20, 25] pointed out that the power law can give a good fit but only over a limited range of pressures and the quadratic equation should be used in preference to model the behaviour of adventitious openings. However, such conclusion was not supported by research studies carried out by Walker [23, 24] who compared the two equations on extrapolating the results measured at high pressures down to low pressures. It was found that the power law better represented the leakage-pressure relationship for buildings with three different types of leakage pathways. In response to this finding, Chiu [22] conducted a numerical study to further explore the question and concluded that power law only provides a good fit at high pressures and at least 40% difference were observed at low pressures between the two equations.

This study aims to compare these two equations on the accuracy of predicting the leakage at low pressures based on the measurements taken by utilising the steady state pressurisation technique by means of the standard blower door test, i.e. a range of high pressures, 10-63 Pa. These tests were carried out under sheltered environments, where the impact of the outdoor weather condition has a reduced impact on the measurements and therefore offers a clear comparison. According to the aforementioned studies both equations are able to provide a mathematical representation with reasonably good accuracy. It could therefore be considered that further research on assessing the margins of accuracy of one equation versus the other might therefore provide little benefit to practical testing. However, from the authors' perspective, understanding the theoretical background and practical performance between the

two is of high importance because it would allow us to decide which mathematical form to use for flow analysis and practical measurement in the relevant research [26, 27, 28, 29].

## 2. THEORETICAL BACKGROUND AND INTEPRETATION

The measurement of building airtightness can be implemented by recording the rate of supplied airflow that is used to pressurise the building to a required pressure. This measurement is usually done over a range of building pressures to obtain a leakage-pressure relationship, which is then used to describe the building characteristics in the form of a mathematical representation. The widely accepted form is the power law equation, as described by Eq.(5) [23].

$$Q = C \Delta P^n \quad (5)$$

Where,  $Q$  is the required rate of airflow to produce the building pressure difference  $\Delta P$ ,  $C$  is flow coefficient ( $\text{m}^3/\text{s}/\text{Pa}^n$ ),  $n$  is the pressure exponent. The value of  $n$  lies in the range of 0.5-1, governed by the regime of airflow going through the building leaks. To approximately relate it to the flow regime in fluid mechanics, the flow through the building leakage pathways is equivalent to being turbulent when  $n$  is 0.5 and laminar when  $n$  is 1. But in reality, developing laminar flow and turbulent flow usually coexist in the building leaks. That combination of leaks changes the effective pressure exponent and the average value of  $n$  is normally found to be in vicinity of 0.66 [30].

The power law equation has been found to give a reasonably good empirical description of the flow-pressure relationship [31]. Another mathematical representation of the leakage-pressure relationship is the quadratic form [20], which is described by eq.(6).

$$\Delta P = aQ^2 + bQ \quad (6)$$

This equation provides analytic description of the flow through leakage pathways in the building envelope. The first term on the right of eq.(6) represents momentum change, while the second term corresponds to surface friction. This is somehow similar to the power law equation, whose pressure exponent  $n$  provides the indication of flow regime. However, it also provides a relatively clearer description of the flow regime of the flow experienced by the building as it isolates the friction term from the momentum term while in the power law equation the pressure exponent on its own describes the flow regime and it can be also a function of pressure [15]. Therefore, it was believed by Etheridge that the power law equation is less analytic than the quadratic equation.

However, the power law has a high flexibility in representing the leakage-pressure relationship due to the fact that the flow coefficient and the pressure exponent are able to independently govern the magnitude and shape of the leakage-pressure curve. Hence, it inherently provides a good accuracy in the curve-fitting exercise to the leakage-pressure data points obtained in the airtightness measurement.

Considering the theories of the envelope flow had already been discussed in depth by previous researchers and scientists [15, 20, 23], assessing the validity of them is neither the purpose or within the capacity of this paper. This section only aims to understand the envelope flow theoretically from a different perspective and see how both equations differ and correlate with each other.

Figure 1 illustrates typical locations of leakage pathways that are commonly present in a typical UK dwelling. In a house with more functional spaces and services, extra leakage pathways are in existence, such as leaks through crawlspace, basement, boiler flues and air-source/ground source heat pump system. Therefore, building leaks usually come in various types in terms of their geometry and size, which suggests typical building leaks are a mixture of openings with different hydraulic properties.

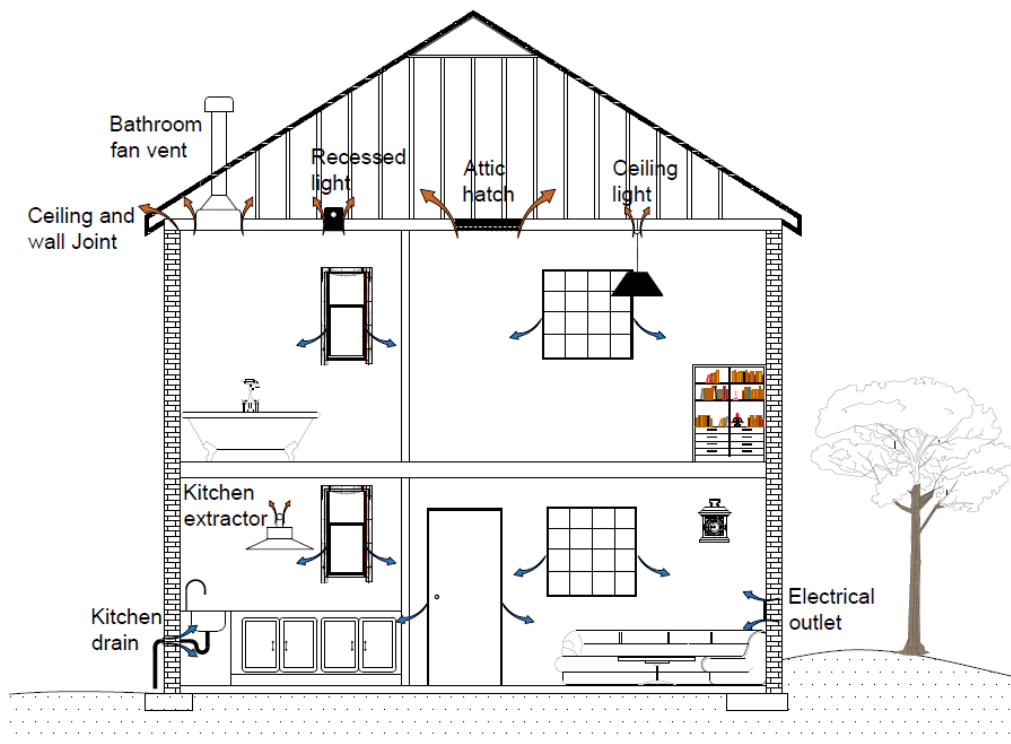


Figure 1 Locations of typical leakage pathways in a residential building [32]

Due to the use of various materials and construction methods [33] as well as ageing process, many different types of leakage pathways can be formed in the envelope of a typical dwelling. They, as three dimensional and irregular openings, not only vary from dwelling to dwelling, but also lead to various leaking routes depending on the workmanship [34]. The characteristic of the building envelope flow can be considered as that arising from an array of individual openings in parallel and in series [20, 23]. For instance, a door often contains two or more different geometries of component opening in parallel [21] and an air vent in a wall can be treated two openings in series. More complex examples are treated by Kronvall [35] where graphical and numerical versions of procedures are described.

Due to the complex nature of building leakage pathways, practical methods are usually adopted to describe the flow characteristics [15, 23, 24] based on simplifications and assumptions. This section aims to interpret the leakage-pressure correlation from the viewpoint of fluid mechanics and revisit current theoretical descriptions to seek for dissimilarities and correlations.

The geometry and dimensions (width and depth) of the leak are useful indicators [36] for characterization due to their direct impact on the hydraulic property of the flow through the leakage pathways driven by pressure difference. They can be generally classified into a number of categories, such as short narrow gap, long narrow gap, convoluted narrow gap, long varying gap, short and sharp-edged opening, short large opening etc. All of them have different hydraulic property due to their different geometries, dimensions, and surface roughness. This is reflected in the hydraulic resistance coefficient. Therefore, when a building is subject to a given pressure difference, different amount of airflows through each individual leakage pathway in the building envelope depending on the corresponding flow resistance. Figure 2 illustrates the schematic diagram of a building leakage pathway with all typical geometries under pressurisation. The resistance components in the flow channel are categorised into various types of hydraulic elements including entry, exit, flow channel with same cross section (C1, C2 and C3), varying geometry such as bend (B1 and B2), constriction (Co) and expansion (E). For instance, a gap between door panel and door frame can be represented by the combination of an entry, C1, B1, B2 and exit. The leakage characteristics of this leakage pathway is highly governed by the one with the highest hydraulic resistance due to its weighted impact on the flow rate under a given pressure difference. However, at the building level where multiple leakage pathways in parallel are subject to a given pressure difference, the leakage characteristic of the building envelope is governed by the one with the smallest hydraulic resistance because most of the flow goes through it. This analogy potentially allows us to determine the type of leakage pathway or even the leakage location more accurately when the construction process becomes standardised in future, such as prefabricated or modular buildings.

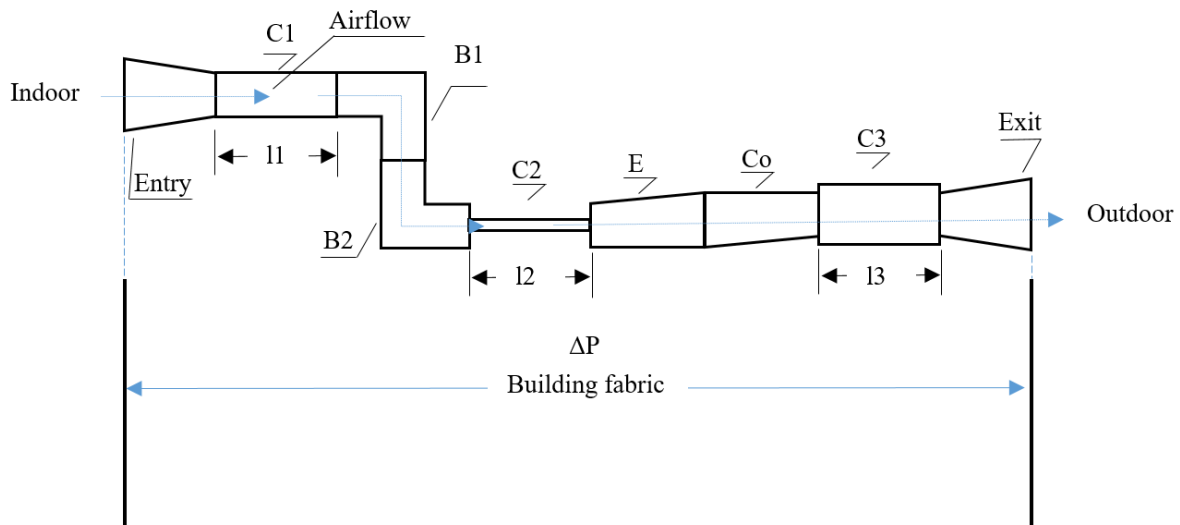


Figure 2 Schematic diagram of a building leakage pathway with typical hydraulic elements (under pressurisation)

Despite the varying dimension and complex geometry of each leakage pathway, it retains sufficient accuracy to presume the resistance components of each leakage pathway consist of all or a combination of the elements shown in Figure 2. The overall flow resistance of the leakage pathway consists of the resistance of the flow through entry, exit, flow channel with varying cross sections such as constriction and expansion, etc. and the resistance caused by the friction between air and the internal surface of the pathway with the same cross section.

Therefore, mathematically the overall pressure drop of the flow through a leakage pathway can be described by eq.(7) according to the Darcy and Weisbach equation [37].

$$\Delta P = \frac{\lambda l}{D_h} \frac{\rho u^2}{2} + \zeta \frac{\rho u^2}{2} \quad (7)$$

Where  $\Delta P$  is the pressure difference across the building envelope in Pascal,  $\lambda$ ,  $D_h$  and  $l$  are the Darcy friction factor (dimensionless), hydraulic diameter (in m) and length (in m) of the leakage pathway in the building envelope,  $\zeta$ ,  $\rho$  and  $u$  are the local resistance coefficient (dimensionless), density (in kg/m<sup>3</sup>) and velocity (m/s) of the flow through the leakage pathway driven by  $\Delta P$ . The first term on the right of eq.(7) represents the pressure loss caused by friction and the second term represents the pressure loss caused by local resistances. Hence, the effective speed of airflow ( $u$ ) through each leakage pathway driven by  $\Delta P$  can be obtained by eq.(8).

$$u = \sqrt{\frac{\Delta P}{\frac{\lambda l}{D_h} \frac{\rho}{2} + \zeta \frac{\rho}{2}}} \quad (8)$$

The Reynolds number ( $Re$ ) of the flow through the leakage pathway takes the form of eq.(9).

$$Re = \frac{D_h \sqrt{\frac{\Delta P}{\frac{\lambda l}{D_h} \frac{\rho}{2} + \zeta \frac{\rho}{2}}}}{\nu} \quad (9)$$

Where  $\nu$  is the kinematic viscosity in m<sup>2</sup>/s.

$Re$ , which only indicates the flow regime of the airflow through each leakage pathway, is determined by the pressure difference that it is subject to, the geometry and dimensions, i.e.  $D_h$ ,  $\lambda$  and  $l$ . In typical building adventitious openings, the Reynolds number tends to stay at a lower level (around 2000) and therefore it is highly unlikely to experience turbulent flow within them [36]. Hence, for instance, long narrow gaps tend to produce laminar flow. For the short wide cracks and gaps, the flow tends to be turbulent due to separated flow at the exit. Greater pressure difference and larger surface roughness can also contribute to the formation of turbulent flow in the leakage pathway.

For the airflow through all the cracks, gaps and adventitious openings in the whole building thermal envelope, it would be crude to simply characterize the flow regime into either laminar, turbulent or transitional because the overall envelope flow consists of flows through a large number of leakage pathways. Each flow has a different Reynolds number, and hence gives different flow regime. However, in order to understand the hydraulic property of the flow

through the building envelope in a simple term, simplifications and assumptions are made herein.

Eq.(7) can be rearranged to Eq.(10) to show the relationship between the established pressure difference across the building envelope and the required airflow rate. It seems to resemble the form of a square law, but it is not a square law relation due to the fact the friction factor ( $\lambda$ ) is determined by flow velocity ( $u$ ) and therefore this equation can be transformed further when  $\lambda$  is represented by the flow velocity through a  $\lambda - u$  relationship.

$$\Delta P = \left( \frac{2\lambda l \rho}{\pi D_h^3} + \zeta \frac{2\rho}{\pi D_h^2} \right) Q^2 \quad (10)$$

Assuming the number of leakage pathways in a building is N, the relationship between the air flow rate through the  $i^{\text{th}}$  leakage pathway and the resulting pressure difference can be described by eq.(11).

$$\Delta P = \left( \frac{\lambda_i l_i}{D_{hi}} + \zeta_i \right) \frac{2\rho}{\pi D_{hi}^2} Q_i^2 \quad (11)$$

Therefore, eq.(11) can be rearranged into eq.(12) and eq.(13) by treating one variable as the function of the other.

$$\Delta P = \frac{\lambda_i l_i}{D_{hi}} \frac{2\rho}{\pi D_{hi}^2} Q_i^2 + \frac{2\rho \zeta_i}{\pi D_{hi}^2} Q_i^2 \quad (12)$$

$$Q_i = \sqrt{\frac{\pi D_{hi}^2}{2\rho} \left( \frac{\lambda_i l_i}{D_{hi}} + \zeta_i \right) \Delta P^{0.5}} \quad (13)$$

In both eq.(12) and eq.(13), the friction factor  $\lambda$  is a dimensionless Darcy friction factor that is determined by the Reynolds number ( $Re$ ) of the flow and surface roughness of each leakage pathway. In the laminar flow ( $Re < 2000$ ), the friction factor  $\lambda$  becomes independent of surface roughness and is a function of  $Re$ , given by eq.(14).

$$\lambda = \frac{64}{Re} \quad (14)$$

In the turbulent flow ( $Re > 4000$ ), this correlation gains dependence on the surface roughness  $\varepsilon$  and its relationship with the  $Re$  also changes. This correlation comes in various forms but all describe  $\lambda$  as a function of  $\varepsilon$ ,  $D_h$  and  $Re$ . A widely used one is Colebrook-White equation, an explicit form of which was described by Swamee-Jain equation [38] for full-flowing circular pipe and is presented herein in eq.(15) as an example.

$$\lambda = \frac{0.25}{\left[ \log \left( \frac{\varepsilon/D_h}{3.7} + \frac{5.74}{Re^{0.9}} \right) \right]^2} \quad (15)$$

When a building experiences laminar flow, eq.(12) changes its form using eq.(14) to quadratic correlation given by eq.(16).

$$\Delta P = \frac{32\rho v l_i}{D_{hi}} Q_i + \zeta_i Q_i^2 \quad (16)$$

Therefore, eq.(12) is able to resemble the quadratic equation described by eq.(6) when a building experiences laminar flow. While, eq.(13) strictly speaking is a square law equation and can be transformed to the power law form with simplified assumptions made [15].

The validity and applicability of both equations have been discussed by the two academic parties [20, 21, 23, 24] with the opposite views on the accuracy of each equation when the openings are in parallel and series. Because the leakage pathways in a typical building are distributed at multiple locations and the pressure distribution within the internal space is uniform during a leakage test, it is reasonable to think the leaks in parallel and in series coexist. But for simplicity, leaks in series can be treated as a single leak with varying cross section, which makes leaks-in-parallel a reasonable approximation of all the leakage pathways in a building. When subjected to the same pressure difference in the air leakage test, the flow through each leakage pathway is determined by its flow resistance.

Therefore, provided the number of leakage pathways in a building envelope is  $N$ , the overall rate of the flow through the building envelope can be given by eq.(17):

$$Q = Q_1 + Q_2 + \dots + Q_i + \dots + Q_N \quad (17)$$

Assuming the resistance coefficient of the  $i^{\text{th}}$  leakage pathway is  $S_i$  when treated as an effective single local resistance that is equivalent to the combination of all the resistance elements in the leakage pathway, the relationship between the pressure difference across the leakage pathway  $\Delta P$  and the corresponding rate of airflow  $Q_i$  can be described by eq.(18) according to the Bernoulli equation.

$$\Delta P = S_i \frac{\rho u_i^2}{2} = \frac{2\rho S_i}{\pi D_h^2} Q_i \quad (18)$$

Where,  $S_i$  can be described by eq.(19)

$$S_i = \frac{\lambda_i l_i}{D_{hi}} + \zeta_i \quad (19)$$

Then the effective resistance coefficient of all the leakage pathways in a building envelope can be expressed by eq.(20) using the electrical analogy.

$$S = \frac{1}{\sum_0^N \frac{1}{S_i}} \quad (20)$$

When the overall envelope flow  $Q$  is considered, the root of eq.(16) can be solved and substituted into eq.(17) to give eq.(21), which is essentially a quadratic relationship.

$$\Delta P = \sum_0^N \zeta_i Q^2 + \sum_0^N \frac{32\rho v l_i}{D_{hi}} Q \quad (21)$$

However, when the envelope flow experiences turbulent or transitional flow, the nonlinear relationship between Darcy friction factor  $\lambda$  and  $Re$  described by eq.(20) would create a new friction element and change the form to being proportional to  $Q^{1.75}$  [36, page 81 and 87]. Therefore, the flow regime has an important bearing on the flow equation for the opening. This makes the quadratic equation less representative of the leakage-pressure correlation when the flow regime is not predominantly laminar. Nevertheless, in a general term, both equations provide a reasonably good mathematical representation of the complex flow through the building envelope.

The accuracy of describing the flow at low pressures by both equations is going to be assessed using experimentally obtained data in a series of testing scenarios where various leakage characteristics were established under sheltered environments.

Based on the aforementioned discussions and the findings reported in previous research, the following questions are established and assessed herein:

- Prediction of the leakage at low pressure using both equations and comparison with the measured data.
- Comparison of curve fitting to the leakage-pressure data points using both power law and quadratic equations at low pressure, high pressure and full range, respectively.

- Assess the relationship between the pressure level and pressure exponent and check if this finding agrees with Etheridge's theory on the impact of the pressure level to the pressure exponent.
- Understanding of hydraulic properties of the envelope flow based on both equations.

### 3. METHODOLOGY

There is no precise definition of high or low pressures in the measurement of building air leakage and they overlap to some extent [36]. For the comparison purpose, the low and high pressures are taken as 0-10 Pa and 10-60 Pa, respectively. Leakage measurements in an extended pressure range were taken in two sets of air leakage tests [39, 40] performed independently in two chambers of different sizes, both of which were enclosed by a larger building to minimize the impact of outdoor weather conditions. The study presented in this paper is drawn from test results of these two different studies where the primary objective for testing in these chambers was to compare the standard blower door method and the novel Pulse technique on the measurement of chamber leakage under sheltered conditions. For that comparative testing of the two air leakage test methods it was necessary for such tests to be performed in an environment where the impact of outdoor weather conditions was minimized and therefore measurements at low pressures using the blower door method was feasible. In this study, the blower door measurements in an extended pressure range taken in both studies are utilised to compare the accuracy of the power law and quadratic equations in predicting the leakage at low pressures using the measured leakage at high pressures. However, it should be noted that due to the construction of these indoor chambers, typical leaks found in traditional building construction are not present within the structure. Therefore, leakage points had to be introduced and therefore due to the nature of these intended openings the setup herein may only provide insights into the scenarios where turbulent flow is predominant in the envelope flow. The two chambers introduced herein are named as chamber 1 and chamber 2. Test scenarios in chamber 1, denoted as Test 1 and test scenarios in chamber 2 denoted as Test 2.

#### 3. 1. Test equipment and chambers

Chamber 1, in which test 1 was performed, is an environmental chamber built inside a large two-storey building at BSRIA Ltd, UK. The chamber envelope, made of insulated cold-store panels, has dimensions of 6.0 m×4.6 m×7.2 m (L×W×H) with a 50 mm wall thickness. The doors in monitoring room and observation room were left open with the air supply, extract and instrumentation holes sealed during testing. The other two walls were exposed to the interior of the sheltering building.

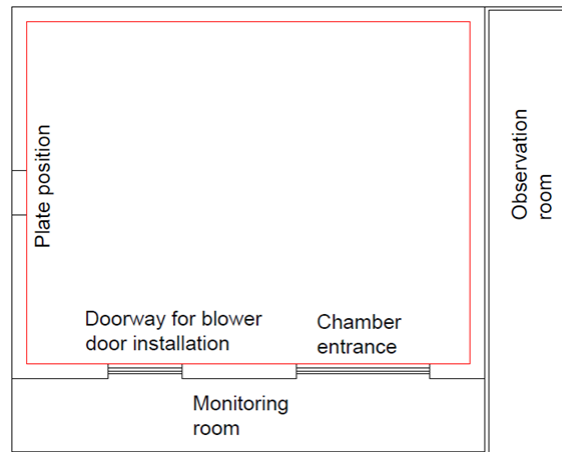


Figure 3 Chamber 1 for testing (the photo is not included herein due to confidentiality) [40]

There are three doors in the chamber envelope, a main entrance door and two smaller doors. The main entrance door was used for access while the small doors were used for the installations of the blower door unit and a compressed-fibreboard (MDF) sheet. In the sheet, plates with different openings were mounted to provide tests with different leakage characteristics and levels. The chamber plan is shown in Figure 3 with the test space indicated by the red rectangle, which is a cuboid space. The installations of the testing plate and blower door unit are shown in Figure 4.

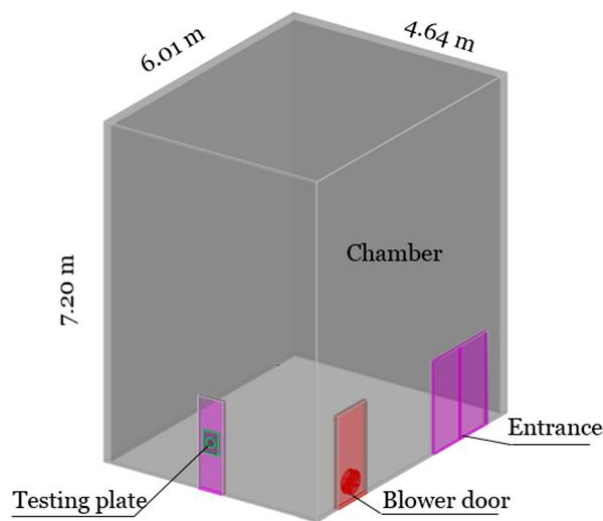


Figure 4 Setup of the test equipment in the chamber [40]

The air leakage of the chamber was tested using the blower door test in two different approaches, one taking measurements in the typical pressure range of 10-60 Pa to comply with the ATTMA technical standard L1 [41], and a non-standard route which takes the readings of the chamber pressure down to 4Pa, i.e. the aforementioned extended pressure range.

Chamber 2, as shown in Figure 5, was sheltered in a large detached building and has dimensions of 4.0 m×2.0 m×2.0 m (L×W×H), giving a volume of 16 m<sup>3</sup> and an envelope area of 40 m<sup>2</sup>. The volume ratios of chamber 1 and chamber 2 to the corresponding sheltering buildings are about 1:20 and 1:100, respectively.



Figure 5 Chamber 2 for testing

Duct Blaster B (DBB), a low-range Minneapolis blower door unit manufactured by ‘The Energy Conservatory’ in the United States, was used in both studies. As shown in Figure 6 and Figure 7, DBB comprised of an adjustable doorframe, a flexible canvas panel, a variable-speed fan, and a DG700 pressure-flow gauge, is set up in both chambers. However, in chamber 2, the flexible canvas panel was replaced by a rigid wooden panel to minimise the impact of blower door installation to the chamber leakage considering the volume of chamber 2 is much smaller than typical dwellings.



Figure 6 Setup of DBB in chamber 1 [40]

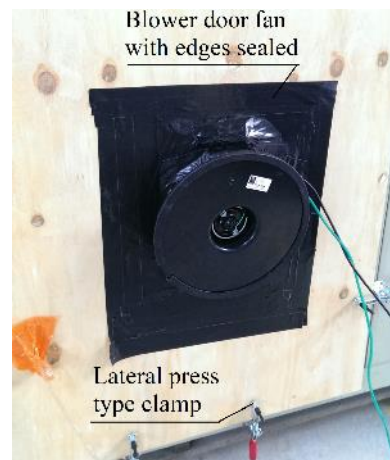


Figure 7 Setup of DBB in chamber 2

### 3. 2. Setup and test arrangement

In chamber 1, 8 fibre-board plates with two thicknesses and four different openings were prepared to provide different leakage characteristics and levels as shown in Table 1. By modifying plates 2 and 3, three additional plates were produced to provide testing scenarios with varied leakage characteristics on top of the 8 scenarios. This was achieved by adding a long air duct to plate 2 and modifying the openings in plate 3 with tape and tightly packed straws. The details for these modifications are listed in Table 2, therefore giving 11 testing scenarios overall.

Table 1 Specifications of testing plates [40]

Scenario	Plate No.	Thickness (mm)	Description	Measured Area (cm <sup>2</sup> )
----------	-----------	----------------	-------------	----------------------------------

1	1	18	Blank plate	0
2	2	18	Circle	318
3	3	18	Four squares	315
4	4	18	Slots	230
5	5	50	Circle	308
6	6	50	Four squares	307
7	7	50	Slots	329
8	8	50	Angled circle	381

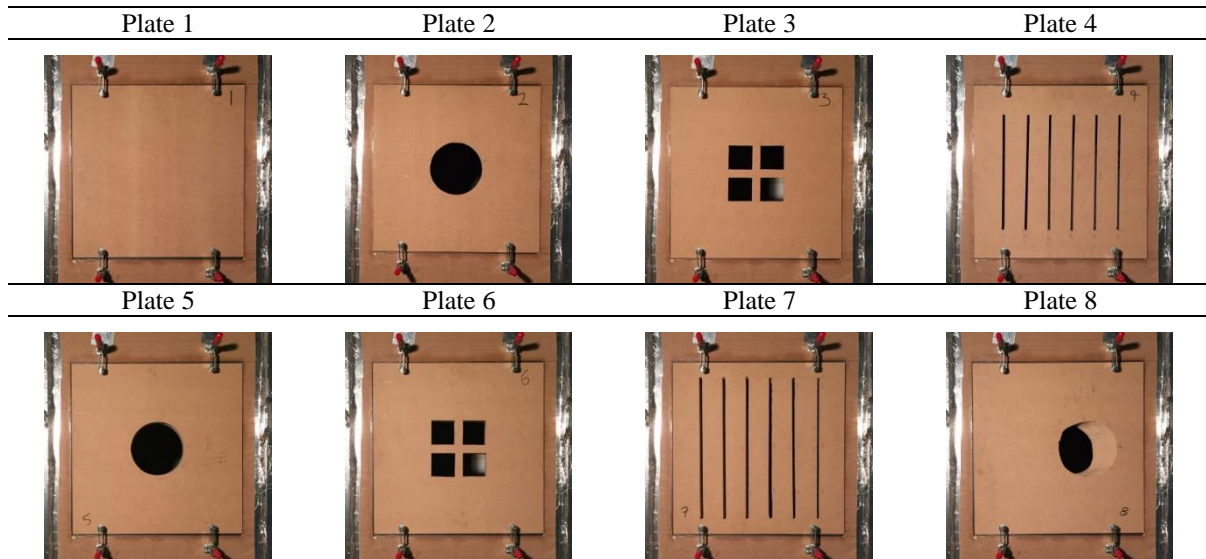


Table 2 Additional testing scenarios with modifications made to plates 2 and 3 [40]

Plate No.	9	10	11
Scenario	9	10	11
	A 410 mm circular duct is added	Three squares were sealed	Straws in one square with others sealed

Modification



The individual testing plates were installed into the chamber envelope by means of an MDF panel sealed into a doorway. This MDF panel as shown in Figure 8, had a square opening with rubber gaskets installed along its edges. A testing plate could therefore be compressed against these gaskets to achieve an airtight installation. Four lateral press type clamps were used to compress the test plate against the gaskets to achieve easy, repeatable and airtight installation.

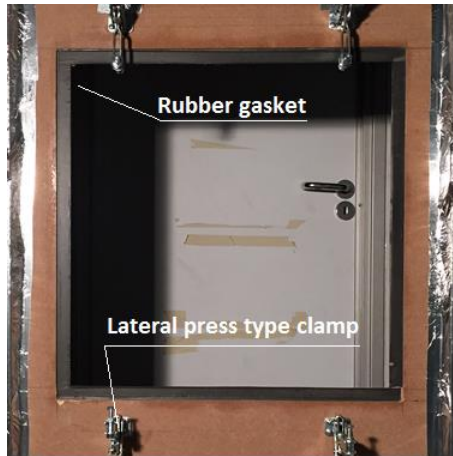
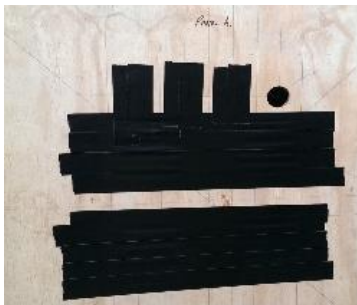
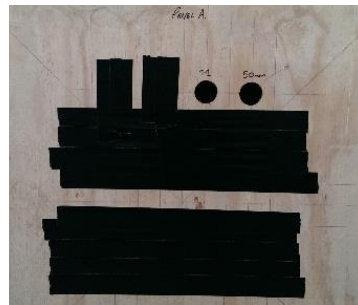


Figure 8 Frame design for assembling the plates [40]

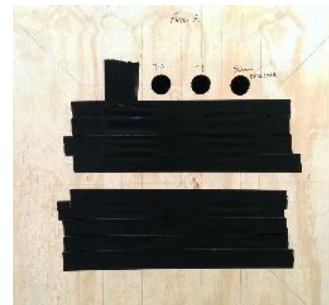
In chamber 2, eight different testing scenarios were established by sealing up various combinations of openings using the two testing plates (A+B). Figure 9 shows how the eight testing scenarios were prepared using sealing tapes. Each testing scenario was named according to the testing order, i.e. starting from scenario T0 and ending with scenario T7. For instance, the first blower door tests were carried out in scenario T0. After the scenario T0 was completed, a piece of sealing tape was removed to introduce one more opening to the scenario T1, and this testing procedure was repeated until the scenario T7 was completed.



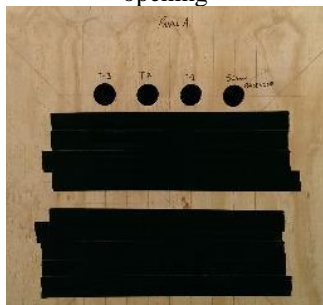
Baseline (T0): Panel A – 1×circular opening



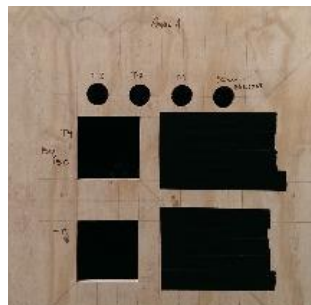
T1: Panel A – 2 circular openings



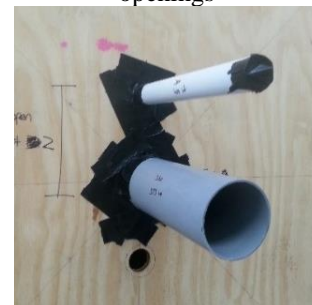
T2: Panel A – 3 circular openings



T3: Panel A – 4 circular openings



T4: Panel A – 4 circular openings plus 2 square openings



T5: Panel B (White blocked grey open)



T6: Panel B (both pipes open)

Figure 9 Testing scenarios in the small chamber

#### 4. RESULTS AND DISCUSSIONS

Due to being sheltered in a large building, it became possible in both chambers to test the leakage over a range of pressure (approx. 4-60 Pa) that is wider than that obtained in a standard blower door test (in a range of approx. 10-60 Pa) where the impact of environment conditions would have not been sheltered.

In order to assess the accuracy of both equations on representing the leakage at low pressure, the data points obtained in the standard blower door tests are fitted with both power law and quadratic equations. Then the leakage at low pressure (4-10 Pa) is calculated using the equations derived in the curve fitting and compared with the measured values. To illustrate how that is done, Figure 10 and Figure 11 show the curves fitted to the points measured at high pressures (10-63 Pa) in the scenario 1 (chamber 1) using both equations with the measured low-pressure points alongside. Both power law and quadratic curves have been fitted to the measurements in both high pressure and full range. As indicated by the R-squared values, both equations give an excellent coefficient of determination at high pressure and in the full range. The extended trend lines of both fitted curves seemingly give a reasonably accurate projection at low pressures. The overall error in obtaining the air leakage rate using both equations has also been given in Figure 12 when the instrumentation accuracy and model error are accounted for, more details on how they are derived are introduced in error analysis in section 5. The overall error lies in 3.0%-8.82% and 3.1%-3.45% when the quadratic equation and power law equation are used to represent the leakage-pressure relationship in the full pressure range, respectively. Interestingly, both equations give a similar overall error when the pressure is in 10-60 Pa as indicated in Figure 12. But in the pressure of interest, i.e. in low pressure range (1-10 Pa), the quadratic equation provides an overall error that is 5.4% greater than that given by the power law equation. Considering the instrumentation accuracy is the same, this finding suggests the quadratic equation experiences higher modelling error at low pressures than the power law equation in this scenario.

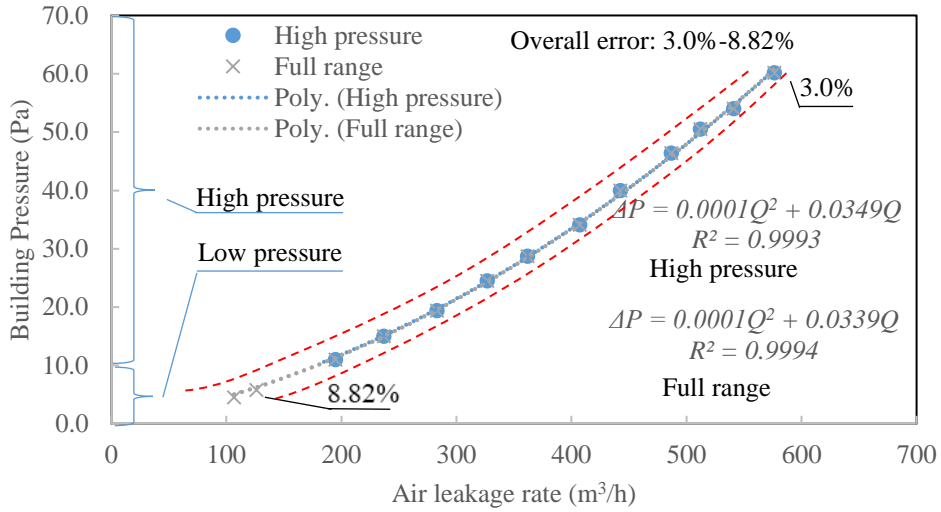


Figure 10 Curve fit with the quadratic equation (scenario 1 in chamber 1)

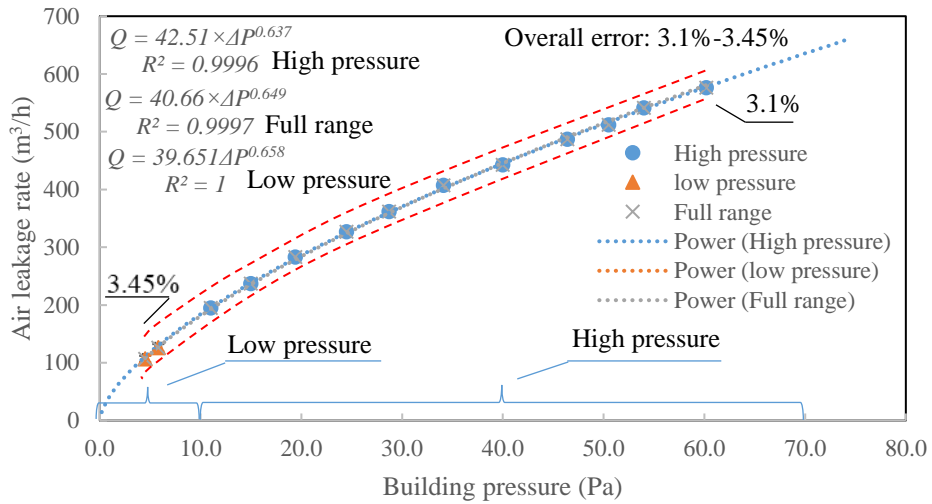


Figure 11 Curve fit with the power law equation (scenario 1 in chamber 1)

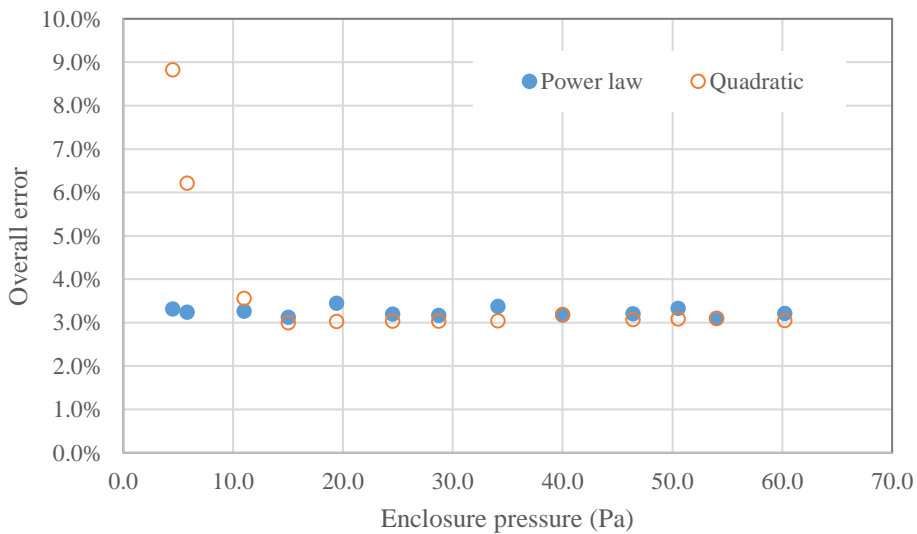


Figure 12 Overall error in obtaining leakage rate at different pressure using power law and quadratic equations (plate 1 in chamber 1)

Table 3 lists coefficients for both equations with 95% confidence intervals obtained by fitting the curves to the points measured at high pressure and the relative percentage difference between predicted value ( $Q_p$ ) using either equation and the measured values ( $Q_m$ ) at low pressures, as described by eq.(22):

$$RPD = \frac{Q_p - Q_m}{Q_m} \quad (22)$$

Where,  $RPD$  is the relative percentage difference between  $Q_p$  and  $Q_m$ .

Both predictions deviate from the measured values by less than 10%, but the power law equation provides a better accuracy in the prediction by up to 5.7%. As indicated by the pressure exponent ( $n$ ) which is below 0.6 in most of the scenarios, the flow regime showed the tendency of turbulent flow except scenario 1 and 11, where a blank test plate and a plate with small opening that has high aspect ratio were present, giving a pressure exponent close to 0.66 identified by Orme [30]. This arrangement provided two different leakage characteristics for testing, i.e. adventitious leakages in the chamber envelope and in combination with manually introduced well-defined opening.

Table 3 Derived equation coefficients (with 95% confidence intervals) and comparison of prediction at low pressures (plate 1 in chamber 1)

Equation	Power law			Quadratic		
	$C$	$n$	$R^2$	$a$	$b$	$R^2$
Coefficients	42.51	0.637	0.9996	0.000126	0.0333	0.9993
Confidence limit (95%)	43.90	0.646	$RPD$	0.000132	0.0359	$RPD$
	41.16	0.628	(-9.6%)-(-6.6%)	0.000119	0.0307	3.3%-3.8%

$RPD$ : stands for the relative percentage difference between predicted leakage and measured leakage, as defined in eq.(22).

For other plates, similar coefficient of determinations were obtained and therefore the fitted curves of them are not illustrated for brevity. The equation coefficients with 95% confidence intervals and accuracies of predictions using both equations in all scenarios are summarised in Table 4. It shows both equations are able to provide an accurate description of leakage measurements and agrees with the finding of a previous research by Etheridge [47], who stated both equations are able to provide a good fit to a network of openings in buildings. However, the power law equation provided better accuracy in predicting the leakage at low pressures than the quadratic equation; which echoed the findings reported by Walker et al [23] under a similar setup, where the two equations were compared on extrapolating the results measured at high pressures down to low pressures. The finding showed the power law better represented the leakage-pressure relationship for buildings with three very different leakage characteristics. This suggests the power law, despite a simpler approach, seems to provide a more accurate representation for the case study [20].

Table 4 Accuracy of predictions at low pressures in all test scenarios in the chamber 1

Equation	Power law			Quadratic		
	$C$	$n$	$R^2$	$a$	$b$	$R^2$
Scenario 1	42.51	0.637	0.9996	0.000126	0.0333	0.9993
Confidence limit (95%)	43.87	0.646	$RPD$	0.000132	0.0359	$RPD$
	41.19	0.628	(-9.6%)-(-6.6%)	0.000119	0.0308	3.3%-3.8%

<b>Scenario 2</b>	<b>C</b>	<b>n</b>	<b>R<sup>2</sup></b>	<b>a</b>	<b>b</b>	<b>R<sup>2</sup></b>
	125.72	0.562	0.9993	0.000032	0.0081	0.9987
<b>Confidence limit (95%)</b>	130.74	0.574	<b>RPD</b>	0.000034	0.0100	<b>RPD</b>
	120.89	0.551	(-0.1%)-0.3%	0.000030	0.0062	(-12.5%)-(-5.9%)
<b>Scenario 3</b>	<b>C</b>	<b>n</b>	<b>R<sup>2</sup></b>	<b>a</b>	<b>b</b>	<b>R<sup>2</sup></b>
	129.97	0.558	0.9991	0.000031	0.0076	0.9987
<b>Confidence limit (95%)</b>	135.67	0.570	<b>RPD</b>	0.000033	0.0094	<b>RPD</b>
	124.50	0.546	(-0.2%)-1.4%	0.000029	0.0059	(-10.2%)-(-5.5%)
<b>Scenario 4</b>	<b>C</b>	<b>n</b>	<b>R<sup>2</sup></b>	<b>a</b>	<b>b</b>	<b>R<sup>2</sup></b>
	120.28	0.555	0.9962	0.000037	0.0084	0.9966
<b>Confidence limit (95%)</b>	131.65	0.529	<b>RPD</b>	0.000041	0.0120	<b>RPD</b>
	109.89	0.581	1.1%-1.5%	0.000033	0.0048	(-11.8%)-(-5.7%)
<b>Scenario 5</b>	<b>C</b>	<b>n</b>	<b>R<sup>2</sup></b>	<b>a</b>	<b>b</b>	<b>R<sup>2</sup></b>
	134.69	0.548	0.9982	0.000032	0.0068	0.9983
<b>Confidence limit (95%)</b>	143.57	0.566	<b>RPD</b>	0.000034	0.0093	<b>RPD</b>
	126.37	0.530	2.0%-4.8%	0.000029	0.0043	(-8.4%)-(-4.5%)
<b>Scenario 6</b>	<b>C</b>	<b>n</b>	<b>R<sup>2</sup></b>	<b>a</b>	<b>b</b>	<b>R<sup>2</sup></b>
	136.32	0.550	0.9988	0.000031	0.0064	0.9989
<b>Confidence limit (95%)</b>	143.16	0.564	<b>RPD</b>	0.000033	0.0084	<b>RPD</b>
	129.81	0.536	1.2%-5.6%	0.000029	0.0045	(-5.6%)-(-4.2%)
<b>Scenario 7</b>	<b>C</b>	<b>n</b>	<b>R<sup>2</sup></b>	<b>a</b>	<b>b</b>	<b>R<sup>2</sup></b>
	147.31	0.561	0.9994	0.000024	0.0064	0.9994
<b>Confidence limit (95%)</b>	151.98	0.571	<b>RPD</b>	0.000025	0.0077	<b>RPD</b>
	142.78	0.551	2.1%-2.4%	0.000023	0.0052	(-7.9%)-(-3.2%)
<b>Scenario 8</b>	<b>C</b>	<b>n</b>	<b>R<sup>2</sup></b>	<b>a</b>	<b>b</b>	<b>R<sup>2</sup></b>
	105.70	0.561	0.9991	0.000045	0.0095	0.9984
<b>Confidence limit (95%)</b>	109.96	0.573	<b>RPD</b>	0.000048	0.0119	<b>RPD</b>
	101.60	0.549	1.3%-4.5%	0.000042	0.0071	(-8.7%)-(-4.9%)
<b>Scenario 9</b>	<b>C</b>	<b>n</b>	<b>R<sup>2</sup></b>	<b>a</b>	<b>b</b>	<b>R<sup>2</sup></b>
	153.61	0.554	0.9991	0.000023	0.0060	0.9992
<b>Confidence limit (95%)</b>	160.66	0.567	<b>RPD</b>	0.000025	0.0076	<b>RPD</b>
	146.87	0.541	(-1.2%)-0.3%	0.000022	0.0044	(-10.4%)-(-6.1%)
<b>Scenario 10</b>	<b>C</b>	<b>n</b>	<b>R<sup>2</sup></b>	<b>a</b>	<b>b</b>	<b>R<sup>2</sup></b>
	71.09	0.572	0.9979	0.000091	0.0145	0.9968
<b>Confidence limit (95%)</b>	76.70	0.594	<b>RPD</b>	0.000099	0.0191	<b>RPD</b>
	65.89	0.551	1.8%-5.1%	0.000083	0.0099	(-0.8%)-0.8%
<b>Scenario 11</b>	<b>C</b>	<b>n</b>	<b>R<sup>2</sup></b>	<b>a</b>	<b>b</b>	<b>R<sup>2</sup></b>
	47.87	0.640	1	0.000098	0.0292	0.9997
<b>Confidence limit (95%)</b>	48.36	0.643	<b>RPD</b>	0.000102	0.0310	<b>RPD</b>
	47.37	0.637	1.0%-3.8%	0.000093	0.0273	(-9.4%)-(-7.5%)

**RPD**: stands for the relative percentage difference between predicted leakage and measured leakage, as defined in eq.(22).

For the power law equation, the flow through building leaks can be considered laminar when the pressure exponent is 1 and turbulent when it is 0.5. In reality, the pressure exponent always lies at somewhere between these two extreme ends due to the aforementioned fact that the flow through the building envelope consists of various types of flows due to the presence of leaks in different types. There is no clear threshold in the pressure exponent that can be used to determine the exact regime of the flow occurring through the building envelope but only indicate the tendency of the flow regime. However, Wolf [42] characterised the type of leakages individually that are commonly seen in residential buildings. The pressure exponent of leakages, experimentally measured individually in a lab, ranged from 0.524 in a light switch to 0.929 in vertical sheathing-to-stud. If an effective pressure exponent is to be used to describe the leakage characteristic of building leakage pathways, it should lie within this range but its value depends on the proportion of each leak type. In this study, the proportion of each

introduced known opening in the overall envelope leakage in both tests can be calculated from the blower door test result of each scenario, as listed in Table 5. Therefore, by introducing the known openings, the  $n$  value is decreased and moves towards 0.5 (except scenario 11 in test 1), which suggests the proportion of short and sharp-edged opening is increased. The introduced opening represents at least 50% of the overall chamber leakage in most scenarios in both tests, this is especially so in the test 2 where the introduced opening stands for most of the chamber leakage. Therefore, the leakage characteristics of the introduced testing scenarios mainly represents the cases where the predominant leakages are short and sharp-edged.

Table 5  $n$  value and proportion of introduced openings in the overall chamber leakage in test 1 and 2

	<b>Scenario</b>	<b>1</b>	<b>2</b>	<b>3</b>	<b>4</b>	<b>5</b>	<b>6</b>	<b>7</b>
Test 1	<b>ELA (<math>m^2</math>)</b>	0.026	0.057	0.058	0.053	0.058	0.059	0.066
	<b>RPD (%)</b>	n/a	54	55	51	55	56	61
	<b><math>n</math> value</b>	0.627	0.588	0.583	0.606	0.582	0.576	0.578
	<b>Scenario</b>	<b>8</b>	<b>9</b>	<b>10</b>	<b>11</b>			
	<b>ELA (<math>m^2</math>)</b>	0.048	0.067	0.033	0.029			
	<b>RPD (%)</b>	46	61	21	10			
	<b><math>n</math> value</b>	0.595	0.576	0.548	0.631			
<b>Note:</b> scenario 1 in test 1 is the baseline scenario where no known opening is installed;								
<b>ELA:</b> stands for the equivalent leakage area reported in a standard blower door test;								
<b>RPD:</b> stands for the relative percentage difference of the introduced opening in the overall leakage.								
	<b>Scenario</b>	<b>Baseline</b>	<b>1</b>	<b>2</b>	<b>3</b>	<b>4</b>	<b>5</b>	<b>6</b>
Test 2	<b>ELA (<math>m^2</math>)</b>	0.002	0.004	0.007	0.009	0.032	0.013	0.015
	<b>RPD (%)</b>	n/a	50	71	78	94	85	87
	<b><math>n</math> value</b>	0.557	0.533	0.526	0.527	0.515	0.520	0.530

Research carried out by BRE on 35 houses [43] pre- and post-sealing of components indicated in the whole house air leakage, 16% was contributed by the unintended gaps in openable windows and doors, 13% was contributed by loft hatch, window/door surrounds and permanent vents and 71% was contributed by gaps and cracks in the building envelope. This suggests the likelihood that adventitious openings are responsible for the majority of building leakage.

Sherman [1] summarised the key leakage pathways in buildings of different types. The location of the leakage is affected by building geometry and construction method [44], it can also change from building to building. For instance, in multi-floor apartments, it was found there was a lot of background leakage other than the usual leakage pathways [45], balcony door was found to be the main source of leakage in multi-family dwellings [46] and using of plasterboard and wet plastering in masonry builds led to very different leakage levels and types. Hence, the answer to the question of which equation is more suited for mathematically representing the leakage-pressure relationship is not clear-cut considering the complex nature of building leakage pathways.

However, it seems both equations share similarity. Etheridge [47] correlated them by showing how the pressure exponent in the power law equation varies for quadratic equation, as described in eq.(23), which, same as eq.(4), suggests the pressure difference that the building is subject to has impact on the pressure exponent [15, 36].

$$n = \frac{1}{2} \left( 1 + \frac{1}{\left( 1 + 4 \frac{a}{b^2} \Delta P \right)^{\frac{1}{2}}} \right) \quad (23)$$

Where,  $a/b^2$  somehow indicates the ratio of turbulent flow component to the laminar flow component. The higher proportion of turbulent flow is in the envelope flow, the closer the pressure exponent is to 0.5. This same trend is also applicable to the pressure difference that the building envelope is subject to. As shown in Figure 13 which is derived from eq.(23), the pressure exponent is the greatest when the pressure difference is at the lowest level. As the pressure difference increases, the pressure exponent decreases and approaches a stable level. This trend is also reflected in the pressure exponents obtained in the power law curve-fitting to the low pressure data, high pressure data and full range data shown in Figure 11, where the pressure exponent at the low pressure is greatest (0.658), followed by the full range data (0.649) and the high pressure data (0.637). Although they are reasonably close to each other, such trend is shown to be possible considering both pressure exponents at low pressure and in full range lie outside the 95% confidence intervals of that at high pressure, as listed in Table 4. The same results were obtained in other plates but not plotted for the sake of brevity. Figure 14 shows that the difference between power law and quadratic equations at low pressure is close to approximately 10% (for instance at 4 Pa), which falls into the similar range of the results experimentally obtained in Table 4. Taking the plate 1 as an example, the relative percentage difference between the results given by both equations lies in the range of 10.4%-12.9%.

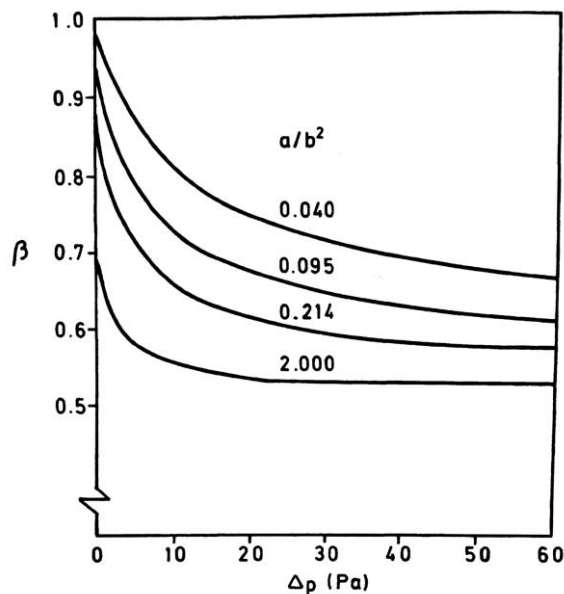


Figure 13 Impact of pressure difference and  $a/b^2$  on the pressure exponent [36] ( $\beta$  is the pressure exponent)

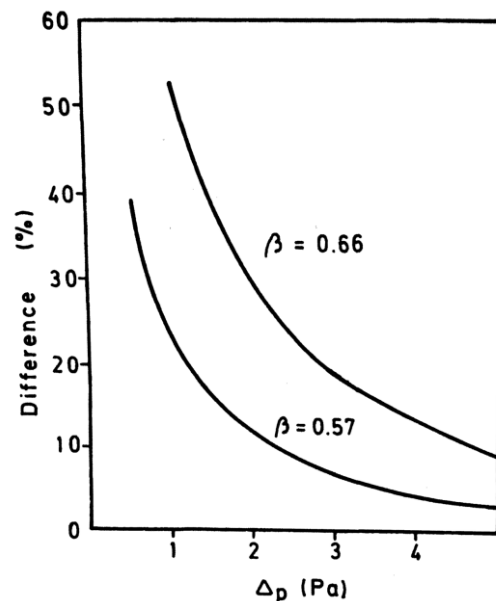


Figure 14 Percentage difference between power law and quadratic equations at low pressure differences after fitting the equations at high pressure difference [36]

With the aid of eq.(23), how the pressure exponent for each scenario varies with the pressure level and the value of  $a/b^2$  can be understood as shown in Figure 15. The values of  $a/b^2$  are grouped into two categories, a low value at 0.10, which is represented by the scenarios with the test plate 1 and test plate 11, and a range of high value in 0.33-0.52, which are represented by the other scenarios where well-defined openings are present. Therefore, both groups are supposed to have different pressure exponents. However, the pressure exponent derived directly from the blower door test in the standard practice is a constant and independent of the pressure difference. In this case, they are 0.64 and 0.55-0.57 for the  $a/b^2$  of 0.10 and 0.33-0.52

respectively. They seem to lie in the variation range of pressure exponent shown in Figure 15 when the chamber is subject to high-pressure differences. Nevertheless, with the aid of  $a/b^2$  and pressure exponent, both equations are able to make an approximate indication and explanation for any change in the flow regime.

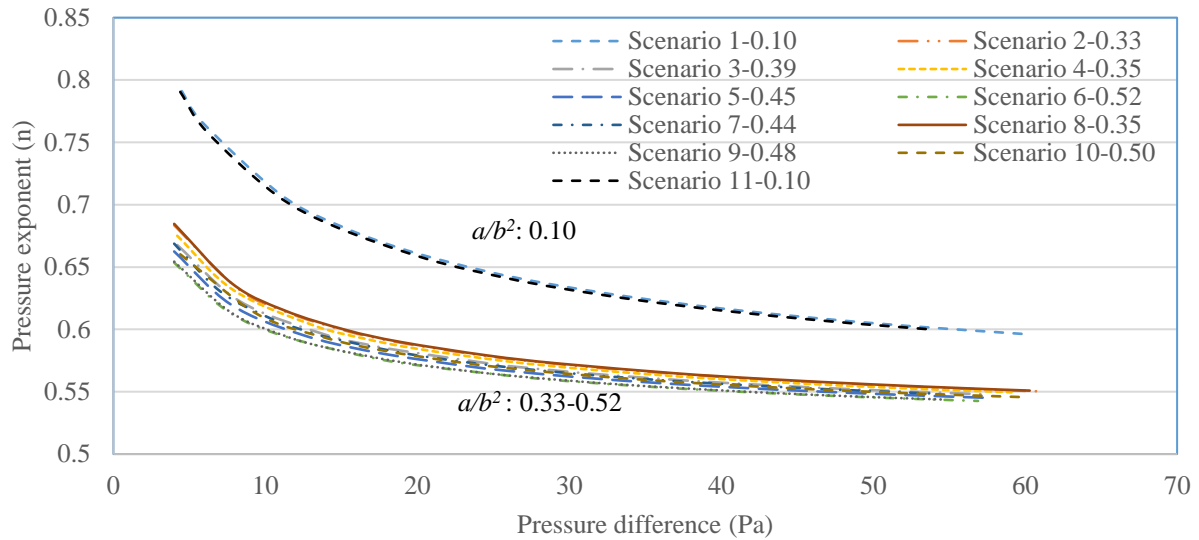


Figure 15 Pressure exponent under different pressure difference in all scenarios (Scenario ID- $a/b^2$ )

Table 6 shows the results of the predictions based on the data experimentally obtained in chamber 2 with 95% confidence intervals. Both equations provided accurate curve fitting with a similar level of coefficient of determination. The predictions of the leakage at low pressures given by both equations have similar level of deviation from the measurements. However, overall a better accuracy (by up to 4%) was achieved with the power law equation despite the opposite trend was observed in scenario 4 and 6. Interestingly, same with the results in chamber 1, the power law equation gave higher leakages at low pressures consistently in comparison with the quadratic equation, which is in agreement with the analysis by Etheridge et al [36, page 107].

Table 6 Accuracy of predictions at low pressures in all test scenarios in the chamber 2

Equation	Power law			Quadratic		
	<i>C</i>	<i>n</i>	<i>R</i> <sup>2</sup>	<i>a</i>	<i>b</i>	<i>R</i> <sup>2</sup>
<b>Baseline</b>	5.35	0.567	0.9996	0.016784	0.1890	0.9985
<b>Confidence limit (95%)</b>	5.64	0.583	<i>RPD</i>	0.018517	0.2576	<i>RPD</i>
	5.08	0.552	1.04%	0.015052	0.1204	-2.68%
<b>Scenario 1</b>	<i>C</i>	<i>n</i>	<i>R</i> <sup>2</sup>	<i>a</i>	<i>b</i>	<i>R</i> <sup>2</sup>
	10.83	0.542	1	0.005519	0.0589	1
<b>Confidence limit (95%)</b>	11.36	0.556	<i>RPD</i>	0.005673	0.0701	<i>RPD</i>
	10.32	0.528	(-0.06%)-2.39%	0.005364	0.0477	(-4.05%)-1.21%
<b>Scenario 2</b>	<i>C</i>	<i>n</i>	<i>R</i> <sup>2</sup>	<i>a</i>	<i>b</i>	<i>R</i> <sup>2</sup>
	16.92	0.525	0.9998	0.002571	0.0372	0.9998
<b>Confidence limit (95%)</b>	17.43	0.534	<i>RPD</i>	0.002669	0.0483	<i>RPD</i>
	16.42	0.517	(-0.91%)-0.83%	0.002474	0.0261	(-5.22%)-(-1.70%)
<b>Scenario 3</b>	<i>C</i>	<i>n</i>	<i>R</i> <sup>2</sup>	<i>a</i>	<i>b</i>	<i>R</i> <sup>2</sup>
	22.10	0.530	0.9999	0.001468	0.0262	1
<b>Confidence limit (95%)</b>	22.56	0.536	<i>RPD</i>	0.001501	0.0313	<i>RPD</i>
	21.66	0.525	(-1.44%)-0.55%	0.001434	0.0210	(-4.07%)-(-0.45%)
<b>Scenario 4</b>	<i>C</i>	<i>n</i>	<i>R</i> <sup>2</sup>	<i>a</i>	<i>b</i>	<i>R</i> <sup>2</sup>
	146.42	0.514	0.9997	0.000040	0.0018	0.9997

<b>Confidence limit (95%)</b>	150.79	0.523	<b>RPD</b>	0.000042	0.0030	<b>RPD</b>
	142.18	0.505	0.22%	0.000039	0.0006	0.01%
<b>Scenario 5</b>	<b>C</b>	<b>n</b>	<b>R<sup>2</sup></b>	<b>a</b>	<b>b</b>	<b>R<sup>2</sup></b>
	204.60	0.529	0.9993	0.000018	0.0022	0.9996
<b>Confidence limit (95%)</b>	214.43	0.542	<b>RPD</b>	0.000019	0.0033	<b>RPD</b>
	195.22	0.515	-1.31%	0.000017	0.0012	-1.37%
<b>Scenario 6</b>	<b>C</b>	<b>n</b>	<b>R<sup>2</sup></b>	<b>a</b>	<b>b</b>	<b>R<sup>2</sup></b>
	293.87	0.510	0.9931	0.000010	0.0006	0.9930
<b>Confidence limit (95%)</b>	332.86	0.546	<b>RPD</b>	0.000012	0.0032	<b>RPD</b>
	259.44	0.474	-1.49%	0.000009	-0.002	-1.19%

RPD: stands for the relative percentage difference between predicted leakage and measured leakage, as defined in eq.(22).

Figure 16 shows how the pressure exponent changes with the achieved pressure difference in the blower door test. Similar to the findings in the chamber 1, the pressure exponent approached a steady level at high pressures and varied significantly at low pressures. However, when the  $a/b^2$  reduced, both the level of pressure exponent and the pressure range over which the pressure exponent has greater gradient increased. Such trend suggests the chamber envelope experienced more laminar flow in the scenario with smaller  $a/b^2$  than other scenarios, which is in agreement with the increased pressure exponent, i.e. smaller  $a/b^2$  implies an increased percentage of laminar flow.

Interestingly, compared to chamber 1, a greater  $a/b^2$  value has been achieved in the tests performed in chamber 2. This is caused by the fact the envelope area of chamber 1 is about 10 times larger than that of the chamber 2, which indicates inherently chamber 1 has greater background leakage than chamber 2 due to the increased surface area. In addition, chamber 2 is modified from a shipping container and consequently has a better envelope integrity. Therefore, the introduced sharp-edged openings installed in the envelope of chamber 2 represent a much greater proportion of the overall chamber leakage and lead to smaller pressure exponent. This is more obvious in scenario 1-6 due to increased effective opening area, where the pressure exponent approaches 0.5.

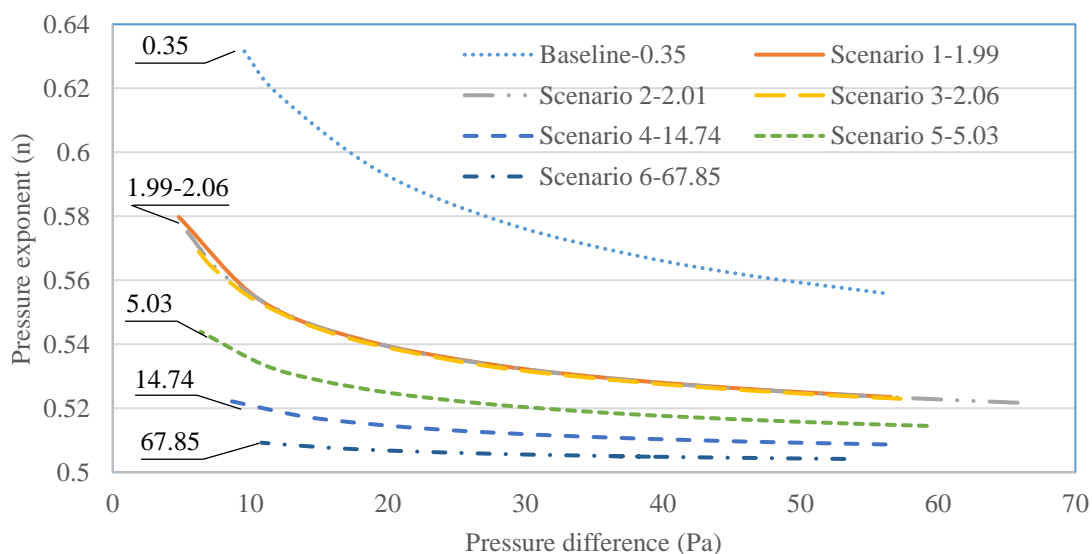


Figure 16 Pressure exponent under different pressure difference in all scenarios in the chamber 2 (Legend annotation explained: Scenario ID- $a/b^2$ )

## 5. ERROR ANALYSIS

The prediction of leakage rate at a pressure level that is outside the range of measurement involves the measurement using instrumentation and subsequent calculation based on a mathematical model that describes the leakage-pressure relationship. When a standard blower door test is performed at high pressure, the main sources of error in obtaining the leakage rate at low pressure include precision error (background noise), the instrumentation error (bias error) and model error [48]. The precision error and instrumentation error fall under the measurement uncertainty or measurement error. Therefore, the error analysis reported herein is focused on the measurement error given by the blower door equipment and model error associated with utilising power law or quadratic equation to describe the leakage-pressure relationship for further calculations. Mathematically, the overall error in obtaining the leakage rate  $\Delta q$  can be described by Eq.(24).

$$\delta q = \sqrt{\delta E^2 + \delta M^2} \quad (24)$$

Where,  $\delta E$  and  $\delta M$  are the resulted errors in leakage rate from measurement and modelling specification, which are treated independently.

The measurement error  $\delta E$  is determined by the pressure-flow gauge that is used to measure the exerted airflow through the fan and corresponding building pressure. The pressure-flow gauge used in both experimental studies is Minneapolis DG700, whose accuracies in measuring the fan airflow and building pressure are listed in Table 7. The error in the measurement of building fan airflow is addressed as  $\delta F$ , which is usually considered to be fixed value independent of the building pressure and equivalent to the measurement error of envelope flow. Therefore, eq.(25) provides the calculation of measurement error of the leakage rate caused by the instrumentation accuracy.

$$\delta E = \sqrt{\delta G^2 + \delta F^2} \quad (25)$$

Where,  $\delta G$  is the error in the quoted leakage rate due to the measurement accuracy of the building pressure.

Table 7 Sources of error in blower door tests under sheltered conditions

Sources of error	Error
Fan airflow, $\delta F$	$\pm 3.0\%$
Building pressure, $\delta p$	$\pm 0.9\%$

$\delta G$  is determined by the combination of the mathematical representation that is used to describe the leakage-pressure relationship and the measurement error of building pressure,  $\delta p$ . The latter in this case includes the instrumentation accuracy and background noise caused by the environmental conditions.

For the power law equation, the measurement error of the air leakage rate at the pressure of  $\Delta P$  can be quantified by eq.(26).

$$\delta G = \frac{(1 \pm \delta p)^n - 1}{1} \quad (26)$$

For the quadratic equation, the measurement error of the air leakage rate at the pressure of  $\Delta P$  can be quantified by eq.(27).

$$\delta G = \frac{\sqrt{b+4a\Delta P(1+\delta p)} - \sqrt{b+4a\Delta P}}{-b + \sqrt{b+4a\Delta P}} \quad (27)$$

$\delta G$  is equal to 0.5% and in the range of 0.02%-0.2% for all the testing scenarios in the pressure range of 4-60 Pa when the power law and quadratic equation is used, respectively. Therefore,  $\delta E$  is predominantly determined by the measurement error of fan airflow  $\delta F$  and calculated to be 3.1% and 3.0% respectively for power law and quadratic.

Regarding the model error  $\delta M$ , it is defined as the standard error of the regression using the mathematical model. The results in all scenarios are listed in Table 8, which shows the power law equation gives slightly smaller error than the quadratic equation.

Table 8 Standard error ( $\delta M$ ) of regression using power law and quadratic equation in both tests

Test	Scenario	1	2	3	4	5	6	7
1	Power law	1.04%	0.80%	0.77%	1.67%	1.31%	1.13%	0.94%
	Quadratic	3.10%	3.67%	1.12%	2.00%	1.65%	1.29%	1.40%
	Scenario	8	9	10	11			
	Power law	1.11%	0.83%	1.35%	0.51%			
	Quadratic	1.46%	1.28%	1.06%	0.70%			
	Scenario	Baseline	1	2	3	4	5	6
2	Power law	0.72%	0.94%	0.59%	0.55%	0.45%	0.90%	1.75%
	Quadratic	1.44%	1.83%	1.63%	1.24%	0.44%	0.98%	1.75%

Using eq.(24), the overall error  $\delta q$  in obtaining the air leakage rate through the blower door measurement and subsequent calculation using power law or quadratic equation are calculated and plotted in Figure 17.

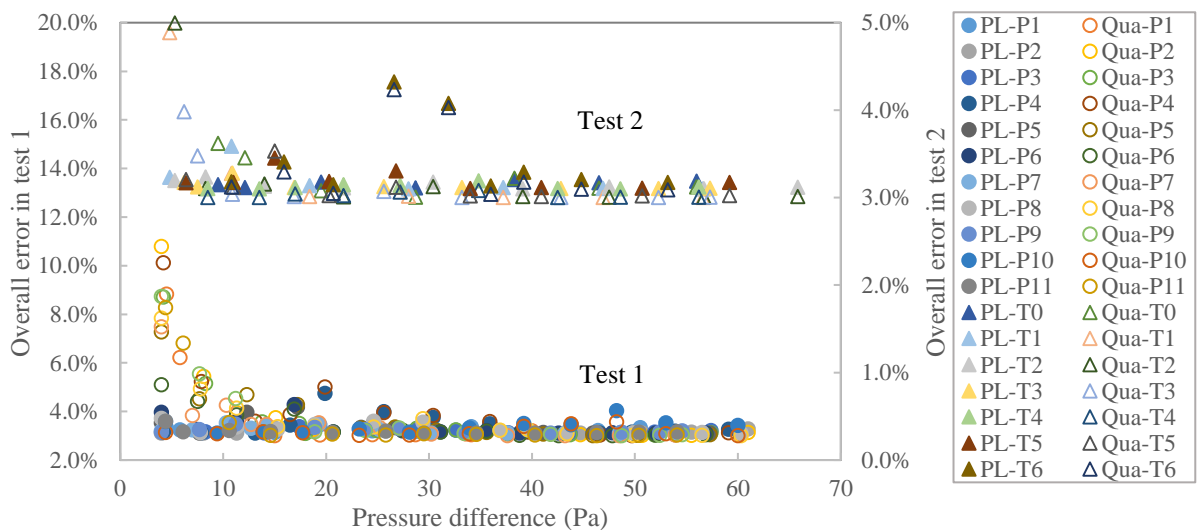


Figure 17 Overall error of the leakage measurement using power law and quadratic equations in both tests (PL: stands for power law equation; Qua: stands for quadratic equation.)

For both equations, all tests have an overall error between 3.0% and 5.0% when the measurement is taken at high pressure, i.e. 10-63 Pa. This stands true for the power law equation even when the measurement pressure lies in the low range, i.e. 1-10 Pa. However,

when the quadratic equation is used, a detrimental effect can be observed in the overall error in both tests at low pressures, i.e. the lower the pressure, the larger the overall error becomes. This suggests the power law provides smaller overall uncertainty in obtaining the leakage at low pressure than quadratic. For the tests performed in chamber No.1, the results listed in Table 4 show extrapolation error incurred in the scenario 5, 6 and 10 was greater than the overall error when the power law equation was used. For the quadratic equation, extrapolation error observed in almost all scenarios except No.10 was greater than the overall error, and the extrapolation error produced with the quadratic equation is up to 6% greater than that given by power law equation. Interestingly, for the tests performed in chamber No.2, all extrapolation error produced with the power law equation is within the overall error, whilst for the quadratic equation, the extrapolation error in scenario 2 was greater than the overall error. Therefore, most of extrapolations produced with the power law equation lies within the overall measurement error, whilst most of extrapolations produced with the quadratic equation have an error that is greater than the overall error, suggesting the power law equation is a more accurate mathematical representation than the quadratic equation in these two case studies.

## 6. CONCLUSIONS

The mathematical representations of the leakage-pressure relationship have been introduced and the theoretical interpretation of the flow through the building envelope has been made from the fluid mechanics' perspective. Based on the assumption that the building leakage pathways consist of a number of leaks in parallel, both power law and quadratic forms can be resembled.

The quadratic equation is able to provide analytic understanding of the problem of interest and the validity of which depends on the presence of laminar flow. Previous research shows that during an air leakage test the building envelope tends to experience laminar flow due to the leakage characteristics of building leakage pathways, which are dominated by the adventitious openings [43]. This can also be attributed to the fact that the likelihood for the flow to fully develop and become turbulent is small [36]. However, short and sharp edged openings are often seen in buildings and such leakage component leads to the formation of turbulent flow through flow separation at exits. The power law equation, as a simplified approach to mathematically represent an empirical relationship for complex physical phenomena, is often used to describe turbulent flow situations [49, 50]. However, research by Sherman showed [15] that it is also able to provide accurate description of the laminar flow situation.

The accuracy of both power law and quadratic equations on predicting the leakage at low pressures have been compared based on the experimentally obtained data under sheltered conditions. The results showed that both equations were able to provide a similar and good accuracy on the curve fitting exercise to the measured data at high pressures and predictions at low pressures. However, it was also found out that the prediction given by the power law equation was more accurate (by up to 6%) than that given by the quadratic equation, which is in agreement with previous experimental investigations by Walker et al [23, 24].

Although the power law equation does not correlate with the geometry of the openings, it provides an accurate curve fitting of the measured leakage-pressure data at various pressure levels, which can be attributed to the flexibility of the equation. For instance, the flow coefficient changes simultaneously to compensate any change in the pressure exponent in order to maintain a good accuracy of curve fitting.

Nevertheless, the results of the tests performed in both chambers showed that both equations were able to provide an accurate indication of the hydraulic property of envelope flow under various scenarios by using the coefficients of both equations (pressure exponent ( $n$  value) and the value of  $a/b^2$ ). The flow regime experienced in both chambers is different from that experienced in a typical dwelling where the flow is much less turbulent. For instance, the average value of pressure exponent shown in typical dwellings is 0.66 [30] but the pressure exponent of all scenarios reported in this study lies below 0.66 with majority of them being below 0.60. Therefore, the proportion of laminar flow experienced by most leakage scenarios (except the baseline scenarios) in this study is much lower than that of typical dwellings and it may change the theoretical assumption on which the quadratic form is based. However, the overall finding in this study is applicable for average dwellings and the ones with large, short and well-defined leakage pathways, i.e. aged, leaky or poorly constructed buildings, which represents approximately 50% of the leakage characteristics of a large data sample reported by Orme et al in [30] (Figure 2.8 on page 52). Future studies on the buildings with more airtight enclosures (such as low carbon or Passivhaus standard buildings) are recommended to see if the findings reported herein stands.

## **ACKNOWLEDGEMENT**

The authors gratefully acknowledge the funding received from: EPSRC IAA. The experimental data used for verifications in this study was obtained in collaboration with BSRIA and Build Test Solutions Ltd in projects supported respectively by European Union's Horizon 2020 research and innovation programme under grant agreement No 637221. ['Built2Spec': [www.built2spec-project.eu/](http://www.built2spec-project.eu/)] and Department for Business, Energy and Industrial Strategy Energy Entrepreneurs Fund Scheme, Phase 5 (EEF5029).

## **REFERENCE**

---

[1] M.H. Sherman, R. Chan

### **Building Airtightness: Research and Practice**

Lawrence Berkeley National Laboratory Report (2004), Report No. LBNL-53356

[2] J. Jokisalo, J. Krunitski, M. Korpi, T. Kalamees, J. Vinaha

### **Building Leakage, infiltration, and energy performance analyses for Finnish detached houses**

Building and Environment 44 (2009) 377-387.

[3] G Raman, K Chelliah, M. Prakash, R.T.Muehleisen

### **Detection and quantification of building air infiltration using remote acoustic methods**

Inter. Noise 2014, Melbourne, Australia. 16-19 November, 2014.

[4] National Institute of Standards and Technology (1996)

### **NIST estimates nationwide energy impact of air leakage in U.S. buildings**

Journal of Research of the NIST 101(3): 413.

[5] S.J. Emmerich., A.K. Persily

### **Energy impacts of infiltration and ventilation in U.S. office buildings using multizone airflow simulation**

IAQ and Energy 98, pp.191-203

[6] Jokisalo, J. Krunitski, M. Korpi, T. Kalamees, J. Vinaha

---

**Building Leakage, infiltration, and energy performance analyses for Finnish detached houses**

Building and Environment 44 (2009) 377-387

[7] H. Ross

**“Air Infiltration,” Lecture at Public Meeting**

DoE, Division of Building and Community Systems, Architectural and Engineering Systems Branch, 21 September 1978.

[8] Kirkwood RC (1977)

**Fuel consumption in industrial buildings**

Building Services Engineer 45(3): 23–31

9] Nevrala DJ and Etheridge DW (1977)

**Natural ventilation in well-insulated houses**

In: Proceedings of International Centre for Heat and Mass Transfer, International Seminar, UNESCO, Volume.

[10] Caffey GE (1979)

**Residential air infiltration**

ASHRAE Transactions 85: 919–926.

[11] Zheng X.F., Cooper E.W., Gillott M., Pasos A.V., Wood C.J.

**A practical review of alternatives to the steady pressurisation method for determining building airtightness**

Renewable and Sustainable Energy Reviews (2020), (accepted for publication).

[12] M. Gillott, D.L. Loveday, J. White, C.J. Wood, K. Chmutina, K. Vadodaria.

**Improving the airtightness in an existing UK dwelling: the challenges, the measures and their effectiveness**

Building and Environment (2016), 95, pp. 227 – 239

[13] M. Nofal, K Kumaran

**Biological damage function models for durability assessments of wood and wood-based products in building envelopes**

Eur. J. Wood Prod. (2011) 69:619–631

[14] Zabel RA, Morrell JJ (1992)

**Wood microbiology: decay and its prevention**

Academic Press, San Diego, p 476

[15] Sherman, M.H.

**A power law formulation of laminar flow in short pipes**

Journal of Fluid Engineering (1992), 114, pp.601-605

[16] J. Boussinesq, Mem. Pres. Acad. Sci. Paris, 23:46 (1891)

[17] L. Schiller, Z. Agnew, Math. Mech. 2:96 (1922).

[18] H. Langharr,

---

## **Steady Flow in the Transition Length of a Straight Tube**

J. Appl. Mech 9:A55 (1942).

[19] E.W. Cooper, D.W. Etheridge

### **Determining the adventitious leakage of buildings at low pressure. Part 1: uncertainties**

Building Serv. Eng. Res. Technol. (2007), 28, pp.71-80

[20] D.W Etheridge

### **A note on crack flow equations for ventilation modelling**

Building and Environment (1998), 33 (5), pp.325-328

[21] D.W. Etheridge

### **Crack flow equations and scale effect**

Building and Environment (1977), 12, pp.181-189

[22] Chiu Y. H., Etheridge D. W. (2002)

### **Calculations and Notes on the Quadratic and Power Law Equations for Modelling Infiltration**

International Journal of Ventilation, Volume 1 No. 1, pp. 65-77

[23] Walker I., Wilson D. and Sherman M. H.

### **A Comparison of the Power Law to Quadratic Formulations for Air Infiltration Calculations**

Energy and Buildings, Vol. 27, No. 3, June 1997.

[24] I.S Walker, D.J. Wilson, M.H. Sherman

### **Does the power law rule for low pressure building envelope leakage?**

Proceedings of 17<sup>th</sup> AIVC Conference, Gothenburg, Sweden. 17-20 September 1996.

[25] D.W. Etheridge

### **Nondimensional methods for natural ventilation design**

Building and Environment (2001), 37, pp.1057-1072

[26] H. Okuyama, Y. Onishi

Reconsideration of parameter estimation and reliability evaluation methods for building airtightness measurement using fan pressurization

Building and Environment (2012), 47, pp. 373-384, doi:10.1016/j.buildenv.2011.06.027

[27] E.W. Cooper, X.F. Zheng, C.J. Wood, M. Gillott, D. Tetlow, S. Riffat, L.D. Simon

### **Field trialling of a pulse airtightness tester in a range of UK homes**

Int. J. Ventilation, 18(1) (2019), pp.1-18.

[28] Zheng X.F., Cooper E., Mazzon J., Wallis, I., Wood, C. J.

### **Experimental insights into the airtightness measurement of a house-sized chamber in a sheltered environment using blower door and pulse methods**

Building and Environment (2019), 162. <https://doi.org/10.1016/j.buildenv.2019.106269>

[29] Zheng X.F., Mazzon J., Wallis I., Wood, C.J.

### **Airtightness measurement of an outdoor chamber using the Pulse and blower door methods under various wind and leakage scenarios**

Building and Environment 2020, <https://doi.org/10.1016/j.buildenv.2020.106950>

- 
- [30] Orme M., Liddament M., Wilson A.  
**An Analysis and Data Summary of the AIVC's Numerical Database**  
Technical Note 44, Air Infiltration and Ventilation Centre, Coventry, 1994
- [31] M.H. Sherman, D. Dickerhoff  
**Air-Tightness of U.S. Dwellings**  
15th AIVC Conference: The Role of Ventilation (1994), Vol. 1, pp. 225-234. (LBNL-35700)
- [32] Zheng X.F., Mazzon J., Wallis I., Wood, C.J.  
**Airtightness measurement of an outdoor chamber using the Pulse and blower door methods under various wind and leakage scenarios**  
Building and Environment 2020, <https://doi.org/10.1016/j.buildenv.2020.106950>
- [33] R.J. Lowe, D. Johnston, M. Bell  
**Airtightness in UK Dwellings: A Review of Some Recent Measurements**  
In Proceedings: The Second International Conference on Buildings and the Environment, Paris, June 9-12, 1997
- [34] D. Wolf, F. Tyler  
**Characterization of air leakage in residential structures—part 1: joint leakage**  
Thermal Performance of the Exterior Envelope of Whole Buildings XII International Conference
- [35] Kronvall J.  
**Air flows in building components**  
Report TVBH-1002, Lund University of Technology, Sweden.
- [36] D. Etheridge, M. Sandberg  
**Building Ventilation: Theory and Measurement**  
Wiley, ISBN: 978-0-471-96087-4, December 1996.
- [37] ASHRAE duct design, Chapter 35, 2005 ASHRAE Handbook-Fundamentals (SI)
- [38] Swamee, P.K., Jain, A.K  
**Explicit equations for pipe-flow problems**  
Journal of the Hydraulics Division (1976). 102 (5), pp.657–664
- [39] Zheng X.F., Smith L., Moring A., Wood C.J.  
**Refined assessment and comparison of airtightness measurement of indoor chambers using the blower door and Pulse methods**  
in Proceedings: 'From energy crisis to sustainable indoor climate-40 years of AIVC', 40th Air Infiltration and Ventilation Centre Conference, Ghent, Belgium, October 15-16, 2019
- [40] Zheng X.F., Cooper E.W., Mazzon J., Wallis I., Wood, C.J.  
**Experimental insights into the airtightness measurement of a house-sized chamber in a sheltered environment using blower door and pulse methods**  
Building and Environment 2019, <https://doi.org/10.1016/j.buildenv.2019.106269>.
- [41] ATTMA Technical standard L1  
**Measuring air permeability in the envelopes of dwellings**  
The Air Tightness Testing & Measurement Association (2016)

---

[42] Wolf D., Tyler F.

**Characterization of air leakage in residential structures-part 1: joint leakage**  
2013 ASHRAE

[43] Stephen RK

**Airtightness in UK dwellings.**

Building Research Establishment (BRE) Information Paper IP/1/00. Watford: HIS BRE Press, 2000

[44] Lowe R.J., Johnston D., Bell M.

**Airtightness in UK Dwellings: A Review of Some Recent Measurements**

in Proceedings: The Second International Conference on Buildings and the Environment, Paris, June 9-12, 1997

[45] Murakami S., Yoshino H.

**Air-Tightness of Residential Buildings in Japan**

in Proceedings: Air Infiltration Reduction in Existing Buildings, 4th Air Infiltration and Ventilation Centre Conference, Elm, Switzerland, September 26-28, 1983

[46] Kovanen K., Sateri J.

**Airtightness of Apartments Before and After Renovation**

in Proceedings: Ventilation and Cooling, 18th Air Infiltration and Ventilation Centre Conference, Athens, Greece, September 23-26, 1997, pp. 117-125.

[47] Etheridge D.W.

**Air leakage characteristics of houses- a new approach**

Building Serv. Eng. Res. Technol. (1984), 5(1), pp.32-36

[48] M. Sherman, L. Palmiter

**Uncertainty in fan pressurisation measurements**

Airflow Performance Conference, ASTM International, West Conshohocken, PA, 1995, pp. 266-283, <https://doi.org/10.1520/STP14701S>

[49] J.W. Jeppson

**Analysis of Flow in Pipe Networks**

Ann Arbor Science, pp. 53-69, (1977).

[50] H. Schlichting

**Boundary-Layer Theory**

(McGraw-Hill 1968) pp 598-602